PCCP

COMMUNICATION

View Article Online
View Journal | View Issue

Cite this: *Phys. Chem. Chem. Phys.*, 2016, **18**, 32664

Received 17th October 2016,
Accepted 15th November 2016

DOI: 10.1039/c6cp07093k

www.rsc.org/pccp

Synthesis and reductive elimination of arylPd(II) trifluoromethyl complexes: a remarkable concentration effect on chemoselectivity†

Song-Lin Zhang* and Zhu-Qin Deng

Reductive elimination from Pd(II) aryl trifluoromethyl complexes is a challenging and elusive step which is accompanied by a number of kinetically more favorable side reactions giving rising to a complex mixture. We report herein the synthesis and isolation of several arylPd(II) trifluoromethyl complexes (2a–c) and study their electronic structures, photophysical properties and reductive elimination reactivities. A remarkable concentration effect on chemoselectivity is observed for thermal decomposition of (Xantphos)Pd(II)(Ar)(CF_3) (2c) that favors the formation of Ar–CF_3 at lower concentrations, but gives increasingly more Ar–Ar homocoupling product to a dominant extent as the concentration of 2c increases. This is solid evidence for the involvement of an intermolecular Ar/CF_3 ligand exchange/Ar–Ar reductive elimination mechanism that has been proposed based on DFT computational studies. The interplay between theory and experiment provides valuable insights into the mechanism and kinetics of the key elementary reaction of reductive elimination at Pd(II), and may thus prompt the design of more efficient Pd-mediated nucleophilic trifluoromethylation reactions.

Transition metal-mediated trifluoromethylation reactions are a useful tool for preparing fluorinated compounds widely used in pharmaceuticals, agrochemicals and organic materials.[1] Particularly, Pd- and Cu-promoted aromatic trifluoromethylation reactions have occupied a dominant position.[2,3] It has been generally accepted that reductive elimination from arylPd(II) trifluoromethyl complexes is a key product-releasing elementary step of the catalytic cycle for Pd-mediated nucleophilic aromatic trifluoromethylation reactions. However, reductive elimination of Ar–CF_3 from arylPd(II) trifluoromethyl complexes with most ancillary ligands is known to be kinetically unfavorable and several byproducts such as Ar–Ar, Ar–F and P–F coupling products are often observed.[4–6] Furthermore, the origins of the byproducts are still elusive and convincing experimental evidence has been scarcely disclosed to fully elucidate the kinetics and mechanisms. It is only in very recent years that limited success has been achieved by Buchwald, Grushin and Shoenebeck *et al.*[5] In their reports, the key point for success is the search for an efficient ancillary ligand due to its unique steric and/or electronic properties to promote the desired Ar–CF_3 reductive elimination.

As part of our continuous efforts on trifluoromethylation reactions, we recently prepared a few key Pd and Cu trifluoromethyl intermediates and investigated their reactivity properties in combination with DFT computational studies.[7–9] The results of our DFT study on the rationalization of the difficulties of reductive elimination from ArPd(II) CF_3 complexes containing an ordinary bisphosphine ligand proposed that bimolecular Ph/CF_3 ligand exchange and subsequent Ph–Ph reductive elimination might be a significant kinetically favorable side pathway for (ethylenediphosphine)Pd(II)(Ph)(CF_3) model complex.[10] Furthermore, for (Xantphos)Pd(II)(*para*-CF_3-Ph)(CF_3) complex, the biomolecular ligand exchange is even exergonic by 4.4 kcal mol^{-1}, giving (Xantphos)Pd(II)$(Ar)_2$ and (Xantphos)Pd(II)$(CF_3)_2$ (Scheme 1). Reductive elimination from (Xantphos)Pd(II)$(Ar)_2$ requires only a low activation barrier of 8.0 kcal mol^{-1}, that is largely lower than the activation barrier of 23.2 kcal mol^{-1} required for direct Ar–CF_3 reductive elimination (Scheme 1).[11] This would give rise to the decreased formation of the desired Ar–CF_3 cross-coupling product and the appearance of a significant bisaryl byproduct.

Inspired by these results, we hypothesized that high concentration of ArPd(II) CF_3 complexes should, in principle, accelerate bimolecular ligand exchange as a result of statistically greater probability of intermolecular collision. This should accordingly promote the formation of bisaryl and simultaneously diminish the formation of Ar–CF_3. Herein, we present, for the first time, solid experimental evidence proving this hypothesis by the amazing observation that the concentration dictates the chemoselectivity of Ar–CF_3 cross-coupling *versus* Ar–Ar homocoupling. It should be emphasized that the concentration effect on the

The Key Laboratory of Food Colloids and Biotechnology, Ministry of Education, School of Chemical and Material Engineering, Jiangnan University, Wuxi 214122, Jiangsu Province, China. E-mail: slzhang@jiangnan.edu.cn; Fax: +86-510-85917763; Tel: +86-510-85917763

† Electronic supplementary information (ESI) available: Experimental details, spectroscopic characterization data, X-ray crystallographic study, general procedure for thermal decomposition of **2c** and DFT computational details. CCDC 1446596. For ESI and crystallographic data in CIF or other electronic format see DOI: 10.1039/c6cp07093k

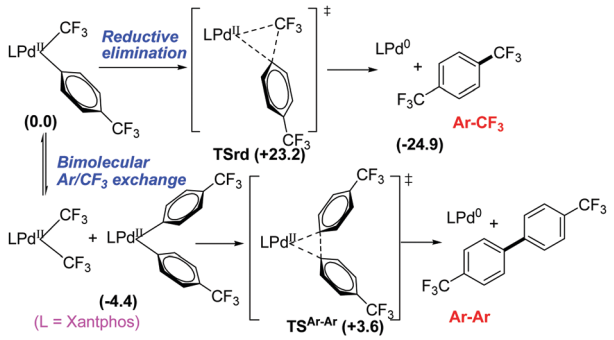

Scheme 1 Direct reductive elimination *versus* bimolecular Ar/CF_3 exchange/Ar–Ar homocoupling for arylPd(II) trifluoromethyl complexes. Values in parentheses are relative free energies in toluene in kcal mol^{-1}.

product chemoselectivity for the reductive elimination of aryl Pd(II) CF_3 complexes has never been reported. The interplay between theory and experiment rationalizes the origins of the Ar–Ar side products and more importantly adds another important mechanistic aspect—namely, concentration effect of the substrate in addition to the ancillary ligand effect—for improving Ar–CF_3 reductive elimination from Pd(II). The valuable and convincing insights into the mechanism and kinetics of the key elementary reaction of reductive elimination at Pd(II) may thus prompt the design of more efficient Pd-mediated nucleophilic trifluoromethylation reactions.

Complexes **1a–c** with the corresponding ligand of bpy, BINAP and Xantphos were prepared by oxidative addition of *para*-trifluoromethylphenyl iodide with $Pd(dba)_2$ in toluene or THF (Scheme 2).[12] Treatment of **1a–c** with CF_3SiMe_3 as the CF_3 source in the presence of AgF at room temperature produced the desired ArPd(II) CF_3 complexes **2a–c**. After workup and recrystallization, **2a–c** were obtained in isolated yields of 69%, 72% and 67%, respectively (for more details on synthesis and purification, please refer to the ESI†).

Complexes **1a–c** and **2a–c** were fully characterized by ^1H, ^{19}F, ^{31}P NMR spectroscopy. For instance, ^{19}F NMR spectra of **1a–c** show only one resonance at *ca.* −62 ppm, attributed to the atromatic CF_3. ^1H NMR spectra are consistent with coordinating bpy, BINAP and Xantphos which are substantially low-field shifted in the aromatic region compared to the free ligands. For **2a–c**, there are consistently two ^{19}F resonances at *ca.* −21 and −62 ppm, corresponding to the metal-bound CF_3 and aromatic CF_3 ligands,

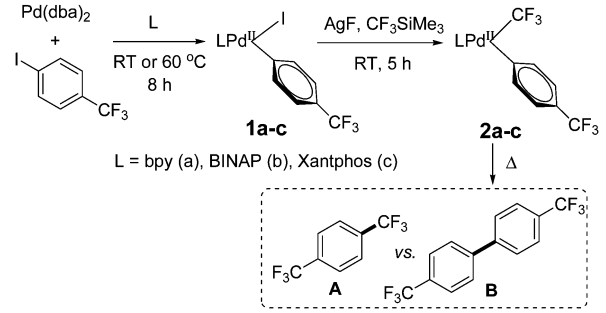

Scheme 2 Synthesis and reactivity of (L)Pd(II)(Ar)(CF_3) complexes **2a–c**.

respectively. Furthermore, there are fine splittings of the two ^{19}F signals in **2b–c** due to the presence of P–F coupling between the bisphosphine P atoms and metal-bound CF_3. Similarly, this P–F coupling is also reflected in the ^{31}P NMR spectroscopy for **2b–c**, leading to fine splitting of the ^{31}P signals (for more details on NMR spectroscopic data, please refer to the ESI†).

The crystal structure of complex **2c** can further be obtained by X-ray crystallographic diffraction analysis.[13] As shown by Fig. 1, complex **2c** clearly shows a square planar geometry with *cis*-orientation of the CF_3 and Ar ligands (Fig. 1) and is in good agreement with ^{19}F and ^{31}P NMR spectroscopy. The Pd–CF_3 and Pd–Ar bond lengths are 2.066(6) and 2.030(6) Å. The CF_3–Pd–Ar bond angle is only 80.7(3) degrees, which should be attributed to the large bite angle of Xantphos that forces the approach of Ar and CF_3 ligands.

To further understand the electronic structure of complexes **2a–c**, UV-vis absorption spectra of **2a–c** were determined (Fig. 2). Complexes **2a–c** all exhibit dominant maximum absorption at *ca.* 228 nm in the UV region that are attributed to π–π* transitions of the ancillary ligands. Notably, **2a** has two additional minor yet significant lower-energy absorption bands at 302 and 314 nm, which are almost negligible for **2b** and **2c**. This suggests significant metal-to-ligand charge transfer for **2a**

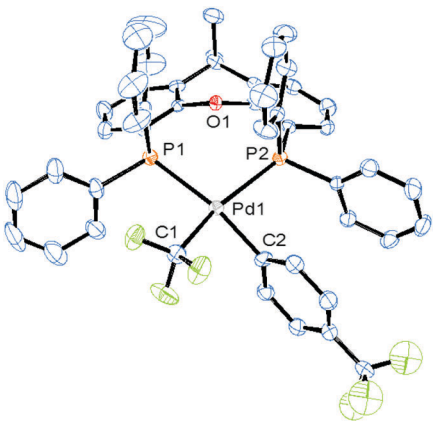

Fig. 1 ORTEP drawing of complex **2c** with thermal ellipsoids at 50% probability. All the hydrogen atoms and solvent molecules are omitted for clarity. Disorders of fluorine atoms are removed for clarity for the aromatic CF_3 substituent.

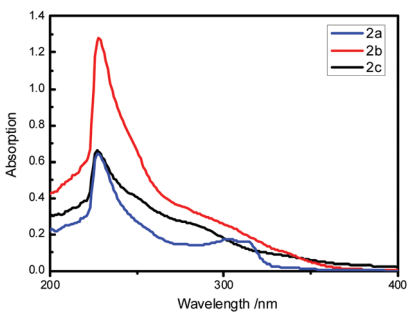

Fig. 2 UV-vis absorption spectra of complexes **2a–c** at a concentration of 10^{-5} M in CH_2Cl_2.

with backdonation of electron from the Pd center to π*-orbitals of the bpy ligand.

Emission spectra of **2a–c** are shown in Fig. 3. In addition to the strong emission at *ca.* 320–330 nm for **2a–c** in the UV range, **2c** exhibits two significant moderate emissions at 413 and 438 nm, corresponding to visible purple emissions. These two minor emissions are however absent for **2a** and **2b**, showing greater intersystem transition of excited states and the resulting stronger phosphorescence emission for **2c**.

Furthermore, DFT computational studies[14,15] were also performed to gain insights into the electronic structures of **2a–c**. As shown in Fig. 4, the HOMO (Highest Occupied Molecular Orbital) of **2c** centers on the Pd $4d_{z^2}$ orbital (Fig. 4a), while the LUMO (Lowest Unoccupied Molecular Orbital) is mainly composed of partial π*-orbitals of Xantphos (Fig. 4b). The HOMO orbital of **2a** is also mainly composed of Pd $4d_{z^2}$ orbital (Fig. 4c), but the LUMO is composed of delocalized π* orbitals across the whole bpy ligand (Fig. 4d). Additionally, the LUMO and HOMO of **2a** are both perpendicular to the molecular coordinating plane and thus parallel well to each other. This match of orbital symmetry should allow a better HOMO/LUMO overlap and thus more favorable metal-to-ligand charge transfer, consistent with the stronger intensity of lower-energy absorption bands around 300 nm for **2a** compared to **2b** and **2c**.

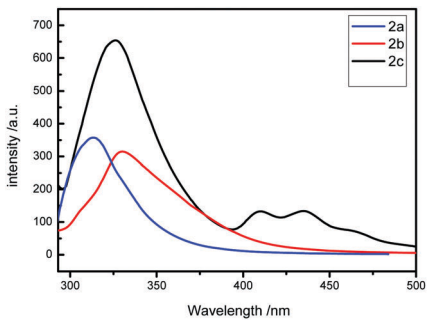

Fig. 3 Normalized emission spectra of complexes **2a–c** at a concentration of 10^{-6} M in CH_2Cl_2 with extinction wavelengths of 297, 279 and 279 nm respectively.

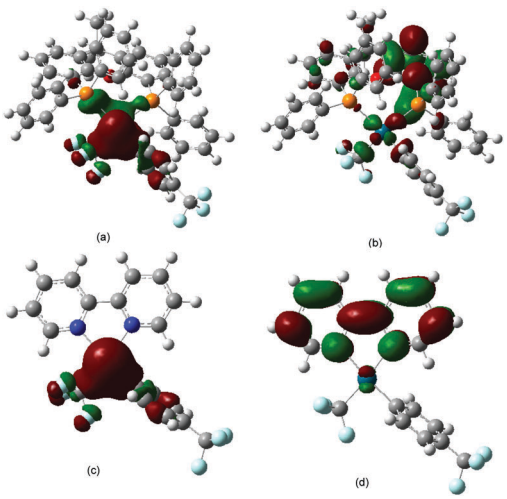

Fig. 4 HOMO and LUMO of **2a** and **2c** with an isovalue of 0.03. (a) HOMO of **2c**; (b) LUMO of **2c**; (c) HOMO of **2a**; (d) LUMO of **2a**.

Table 1 Thermal decomposition of complex **2c** in benzene[a]

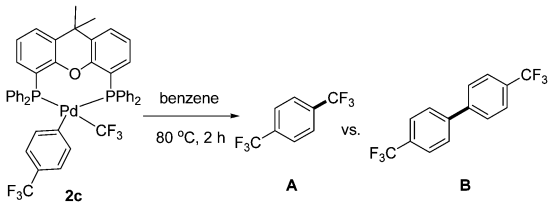

Entry	Conc. (M)	Xantphos	T (°C)	Yield[b] A%	Yield[b] B%
1	0.1	—	40	26	Trace
2	0.1	1 eq.	40	20	Trace
3	0.1	—	80	49[c]	Trace
4	0.1	1 eq.	80	46	Trace
5	0.3	—	80	65	23
6	0.5	—	80	31	32
7	0.7	—	80	24	38
8	1.0	—	80	20	45

[a] Reaction conditions: **2c**, Xantphos (equal to **2c** where present), 4,4′-difluorobiphenyl (equal to **2c**, internal standard, for entries 1–4), benzene (1 mL), under a N_2 atmosphere for 2 hours. [b] Isolated yields using column chromatography. [c] Due to the highly volatile feature of products **A** and **B**, the isolated yields were much lower than the ^{19}F NMR yields (100% as determined by ^{19}F NMR).

Reactivity properties of complex **2c** were further studied by thermally heating benzene solution of **2c** in an oil bath (Table 1).[16,17] As shown by entries 1 and 2, although the conversion was high at 40 °C, the isolated yields of Ar–CF_3 and Ar–Ar were low to trace either in the absence or presence of additional Xantphos. When the temperature was raised to 80 °C, the conversion reached 100% in 2 h as determined by ^{19}F NMR spectroscopy. The major product was Ar–CF_3 with an isolated yield of 49% which was caused by the extremely volatile feature of the Ar–CF_3 product **A** (entries 3 & 4).

It is remarkable to note that as the concentration of **2c** increases, the isolated yield of the cross-coupling product Ar–CF_3 (**A**) reaches a maximum value of 65% at 0.3 M and then gradually decreases (entries 5–8).[18] In sharp contrast, the homocoupling product Ar–Ar (**B**) increases gradually and significantly, up until nearly one-half of the starting Pd(II)(Ar)(CF_3) is converted to Ar–Ar at a high concentration of 1.0 M (entry 8). This observation is consistent with the proposal of the bimolecular ligand exchange/Ar–Ar reductive elimination mechanism since at higher concentrations there is higher probability for bimolecular ligand exchange, and thus more favorable Ar–Ar homocoupling. As far as we know, these results provide for the first time compelling evidence for the involvement of a bimolecular ligand exchange/Ar–Ar reductive elimination mechanism as a potent side pathway competing with the intramolecular direct Ar–CF_3 reductive elimination of Pd(II) aryl CF_3 complexes. These results are believed to be highly important and should be well considered during the design of more efficient nucleophilic aromatic trifluoromethylation reactions.

In summary, several Pd(II) aryl trifluoromethyl complexes **2a–c** are isolated and fully characterized by ^{1}H, ^{19}F and ^{31}P NMR spectroscopy, and X-ray crystallography for **2c**. Electronic structure studies of these Pd(II) complexes are presented, including both UV-vis absorption and emission spectroscopy and DFT computational studies. Finally, reactivity properties of **2a–c** are investigated by thermal heating of their benzene solution. A remarkable concentration effect on the chemoselectivity is observed for **2c**, that is the Ar–CF_3 cross-coupling gradually decreases and simultaneously the bisaryl product increases significantly and steadily as the concentration of **2c** increases. These results provide original and convincing evidence that a bimolecular ligand exchange mechanism should be involved in the reductive elimination of Pd(II) aryl trifluoromethyl complexes, which is consistent with our DFT computational studies and should be valuable for the rational design of more efficient nucleophilic trifluoromethylation reactions.

This study was supported by the National Natural Science Foundation of China (No. 21472068, 21202062) and the Natural Science Foundation of Jiangsu (No. BK2012108).

Notes and references

1 For organofluorine chemistry and applications, see: (*a*) P. Kirsch, *Modern Fluoroorganic Chemistry*, Wiley-VCH, Weinheim, Germany, 2004; (*b*) S. Purser, P. R. Moore, S. Swallow and V. V. Gouverneur, *Chem. Soc. Rev.*, 2008, **37**, 320; (*c*) Y. Jiang, H. Yu, Y. Fu and L. Liu, *Sci. China: Chem.*, 2015, **58**, 673.

2 For general reviews, see: (*a*) M. Schlosser, *Angew. Chem., Int. Ed.*, 2006, **45**, 5432; (*b*) J.-A. Ma and D. Cahard, *Chem. Rev.*, 2008, **108**, PR1; (*c*) V. V. Grushin, *Acc. Chem. Res.*, 2010, **43**, 160; (*d*) T. Furuya, A. S. Kamlet and T. Ritter, *Nature*, 2011, **473**, 470; (*e*) T. Liang, C. N. Neumann and T. Ritter, *Angew. Chem., Int. Ed.*, 2013, **52**, 8214; (*f*) C. Zhang, *Org. Biomol. Chem.*, 2014, **12**, 6580; (*g*) S. Barata-Vallejo, S. M. Bonesi and A. Postigo, *Org. Biomol. Chem.*, 2015, **13**, 11153.

3 For reviews on copper-mediated trifluoromethylation reactions, see: (*a*) O. A. Tomashenko and V. V. Grushin, *Chem. Rev.*, 2011, **111**, 4475; (*b*) S. Roy, B. T. Gregg, G. W. Gribble, V.-D. Le and S. Roy, *Tetrahedron*, 2011, **67**, 2161; (*c*) T. Liu and Q. Shen, *Eur. J. Org. Chem.*, 2012, 6679; (*d*) X. Liu and X. Wu, *Synlett*, 2013, 1882; (*e*) P. Chen and G. Liu, *Synthesis*, 2013, 2919.

4 (*a*) D. A. Culkin and J. F. Hartwig, *Organometallics*, 2004, **23**, 3398; (*b*) V. V. Grushin and W. J. Marshall, *J. Am. Chem. Soc.*, 2006, **128**, 4632; (*c*) For analogous difficult reactions with Ni(II), see: G. G. Dubinina, W. W. Brennessel, J. L. Miller and D. A. Vicic, *Organometallics*, 2008, **27**, 3933.

5 For successful examples of reductive elimination of Ar–CF_3 from Pd(II) centers, see: (*a*) E. J. Cho, T. D. Senecal, T. Kinzel, Y. Zhang, D. A. Watson and S. L. Buchwald, *Science*, 2010, **328**, 1679; (*b*) V. V. Grushin and W. J. Marshall, *J. Am. Chem. Soc.*, 2006, **128**, 12644; (*c*) M. C. Nielsen, K. J. Bonney and F. Schoenebeck, *Angew. Chem., Int. Ed.*, 2014, **53**, 5903.

6 For P–F coupling at Pd and other transition metal centers, see: (*a*) O. Blum, F. Frolow and D. Milstein, *J. Chem. Soc., Chem. Commun.*, 1991, 258; (*b*) S. A. Macgregor, D. C. Roe, W. J. Marshall, K. M. Bloch, V. I. Bakhmutov and V. V. Grushin, *J. Am. Chem. Soc.*, 2005, **127**, 15304; (*c*) V. V. Grushin and W. J. Marshall, *J. Am. Chem. Soc.*, 2004, **126**, 3068; (*d*) S. A. Macgregor, *Chem. Soc. Rev.*, 2007, **36**, 67; (*e*) S. A. Macgregor and T. Wondimagegn, *Organometallics*, 2007, **26**, 1143; (*f*) S. Erhardt and S. A. Macgregor, *J. Am. Chem. Soc.*, 2008, **130**, 15490.

7 S.-L. Zhang, L. Huang and L.-J. Sun, *Dalton Trans.*, 2015, **44**, 4613.

8 S.-L. Zhang and W.-F. Bie, *Dalton Trans.*, 2016, **45**, 17588.

9 S.-L. Zhang and W.-F. Bie, *RSC Adv.*, 2016, **6**, 70902.

10 Computational results showed that bimolecular ligand exchange is endothermic by 2.9 kcal mol^{-1} for $(PH_2CH_2CH_2PH_2)$-Pd(Ph)(CF_3) and subsequent reductive elimination from the resulting $(PH_2CH_2CH_2PH_2)$Pd(II)$(Ph)_2$ has an activation barrier of 12.6 kcal mol^{-1}. Please refer to ref. 7 for more details.

11 For aryl Pd(II) trifluoromethyl complexes with other ligands such as bpy and BINAP ligand, similar results have also been obtained that bimolecular Ar/CF_3 ligand exchange/Ar–Ar homocoupling are kinetically more favorable compared to the direct Ar–CF_3 reductive elimination. Therefore, this competing side pathway should probably be a quite common phenomenon for reductive elimination from aryl Pd(II) trifluoromethyl complexes. Please refer to ESI for more details.†

12 N. D. Ball and M. S. Sanford, *J. Am. Chem. Soc.*, 2009, **131**, 3796.

13 CCDC 1446596 contains the supplementary crystallographic data for complex **2c**.

14 DFT studies were carried out at a level of B97D/SDD-6-311 + g(d,p)//B3LYP/Lanl2dz-6-31g* which has been demonstrated to be a reliable method for treating fluoro-containing Pd complexes in our previous study after great efforts of evaluating and comparing various DFT methods as well as high-accuracy *ab initio* methods. Please see ref. 7 for more results on this issue. For more details on computational methods and optimized structures of stationary points, please refer to the ESI.†

15 For selected other examples of our recent DFT mechanistic studies on Pd-mediated reactions, see: (*a*) S.-L. Zhang, Y. Fu, R. Shang, Q.-X. Guo and L. Liu, *J. Am. Chem. Soc.*, 2010, **132**, 638; (*b*) S.-L. Zhang, L. Shi and Y. Ding, *J. Am. Chem. Soc.*, 2011, **133**, 20218; (*c*) S.-L. Zhang and Z.-L. Yu, *J. Org. Chem.*, 2016, **81**, 57.

16 For detailed reaction procedure and ^{19}F NMR determination of reaction yields, please refer to the ESI.†

17 Complexes **2a** and **2b** were less reactive for reductive elimination under similar conditions, and the isolated yields were low.

18 Due to the extremely volatile features of trifluoromethylated arene products, the values are all at the lower limit due to the severe loss of products during vacuum evaporation of the product solution gathered from column chromatography.